CHAPTER 7

Extratropical transition of tropical cyclones in the North Atlantic

J.L. Evans[1] & R.E. Hart[2]
[1]*Department of Meteorology, The Pennsylvania State University, Pennsylvania, USA.*
[2]*Florida State University, Florida, USA.*

Abstract

Apart from a few early case studies that documented tropical cyclones (TCs) that tracked into the extratropics, it was generally accepted through the 1970s that TCs would decay as they moved out of the tropics. This preconception was challenged in the 1980s. Over the past two decades, a flurry of research on these *extratropically transitioning* TCs has revealed much about their behavior. Here, we discuss extratropically transitioning TCs, beginning from their tropical formation, the conditions under which they evolve, and their spatial and temporal distributions. Case studies are presented and potential indicators of transition, of use to the forecast community, are introduced.

Case studies demonstrate the need for research into the interactions between the evolving TC and an approaching higher latitude trough. Constructive interactions between these systems, when accompanied by a supportive remnant tropical environment, will lead to transition and possibly reintensification of the storm as an extratropical system.

Key results include a late season maximum in the percentage of storms that undergo transition. This late season peak is related to the need for synoptic support for tropical development to intensify cyclones prior to transition, followed almost immediately by a strong baroclinic synoptic energy source as transition occurs. Recognition of key structural changes as the storm transitions has led to the development of a number of indicators of transition currently being tested by the forecast community.

WIT Transactions on State of the Art in Science and Engineering, Vol 23, © 2006 WIT Press
www.witpress.com, ISSN 1755-8336 (on-line)
doi:10.2495/978-1-85312-929-2/07

1 Introduction

Extratropical transition (or ET) is the process by which a tropical cyclone (TC) is transformed into an extratropical cyclone (EC). These EC systems often persist as coherent structures far into the extratropics. In the Atlantic, systems with tropical beginnings have been tracked poleward of 50°N and to the coast of Western Europe, from Spain to Scandinavia (e.g. Bob in 1991, Fig. 1). These systems carry their past with them, as measured by their equivalent potential temperature and potential vorticity signatures. The importance of these latent and dynamic energy sources is explored in the case study example presented in Section 4.

Prior research into ETs in the Atlantic consisted of two papers on a single case in the first half of the 20th century (Tannehill [1]; Pierce [2]), occasional case studies since the 1950s (e.g. Palmén [3]; Kornegay and Vincent [4]; DiMego and Bosart [5, 6]), and a recent rush of studies (e.g. Bosart and Bartlo [7]; Bosart and Lackmann [8]; Thorncroft and Jones [9]; Hart and Evans [10]; Evans and Hart [11]; Jones *et al*. [12]; Atallah and Bosart [13]; Arnott *et al*. [14]). The history of ET research in the Pacific basin is similar (e.g. Sekioka [15, 16, 17]; Matano and Sekioka [18]; Brand and Guard [19]; Harr and Elsberry [20]; Harr *et al*. [21]; Klein *et al*. [22]; Sinclair [23]), with even less attention being paid to the Indian Ocean (Foley and Hanstrum [24]).

Poleward movement of a TC is expected to lead to the decay of the system as it encounters the hostile, strongly sheared environment and cooler waters (or land) of the midlatitudes. The exceptions to this rule are extratropically transitioning TCs. Cyclones undergoing ET may initially weaken as they move into the extratropics, but these systems can reintensify into midlatitude storms that are

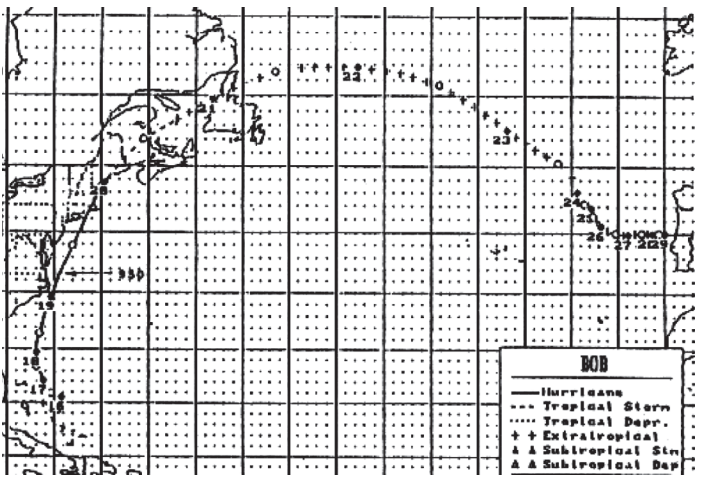

Figure 1: Best track of Hurricane Bob (1991) from August 16–29, 1991. This storm greatly impacted the United States, Canada, and Western Europe. 0000 UTC (1200 UTC) positions are marked with solid (open) circles.

occasionally more intense than their tropical selves (e.g. Irene 1999, Prater-Mayes and Evans [25]; Evans and Prater-Mayes [26]; Agusti-Panareda *et al*. [27]), often traveling at forward speeds of 15–20 m s^{-1}. More commonly, the remnant tropical storm can provide a source of enhanced thermal contrast for the later development of an intense midlatitude storm (e.g. Abraham *et al*. [28]). These systems are often poorly forecast by numerical forecast models (e.g. Rabier *et al*. [29]) and can visit severe weather on the mid-Atlantic and New England coasts of the United States and the Canadian Maritimes, as well as Western Europe (including Scandinavia). Their rapid forward speed, the large size of their gale force wind area and intense asymmetric rainfall region, and the ocean waves they generate provide difficult forecast challenges to the responsible forecast centers around the globe. These intense weather phenomena can exist long after their "tropical storm" status has been discontinued (Abraham *et al*. [28]).

The rapid movement of a transitioning storm and its large area of high wind speeds combine to generate large ocean surface waves and swell (Bowyer [30]; Moon *et al*. [31]). Indeed, MacAfee and Bowyer [32, 33] suggest that the rapid forward speeds of ET storms can result in a "trapped fetch" phenomena in which the storm moves with the fastest growing waves it is generating, providing a much longer period of sustained forcing and resulting in much larger waves than would be possible if the storm were moving at only a few meters per second (as for TCs). Hence, the waves generated by an extratropically transitioning TC can be much larger than the waves generated by a more intense, but slower moving, TC. Enhancement in wave growth occurs only to the right of the track (northern hemisphere; left in the southern hemisphere), in the fastest wind region of the ET storm (where the storm's forward motion is in the same direction as its winds). Bowyer [30] demonstrated this trapped fetch phenomena for the case of Hurricane Luis (1995). Peak waves of over 30 m were generated by Luis and caused extensive damage to the QEII cruise ship. Moon *et al*.'s [31] simulation of detailed wave-wind coupling mechanisms demonstrated skill in modeling the two-dimensional spectra associated with 14 + m significant wave heights produced by the transitioning Hurricane Bonnie (1998) and recognized the challenges in simulating shoaling waves as a storm approaches landfall.

In this chapter, we review the early research and recent advances in the understanding of ET in the North Atlantic basin. We begin in Section 2 with a review of formation (or "genesis") of TCs and their basic structure. A climatology of TCs and ET in the North Atlantic is presented in Section 3. This is followed by an examination of intraseasonal and interbasin variations in ET in Section 4, in which we propose favorable environments for transition. The percentage of tropical storms that undergo ET, that reintensify in their extratropical phase, and those that make landfall are identified. We explore the origins of these systems and their paths to transition. A "typical" ET case study, Hurricane Floyd (1999), is documented in Section 5. In Section 6 we discuss the informal set of criteria that have evolved for diagnosing and forecasting ETs and we introduce an alternative objective approach, the cyclone phase space (CPS) (Hart [34]; Evans and Hart [11]). A brief summary is provided in Section 7.

2 A basic primer on TC formation and structure

According to the World Meteorological Organization (WMO), a TC is a warm-core, nonfrontal, low-pressure system that develops over the ocean and has a definite organized surface circulation. A tropical storm is a TC whose intensity (measured as the maximum sustained surface wind speed) exceeds 63 km h^{-1} (39 mph). In the Atlantic basin, intensity is measured by the peak *one-minute* averaged wind near the center, although the convention followed in the western Pacific and Indian Oceans is for *ten-minute* averaged winds to be used for intensity. A TC is assigned a name once it reaches tropical storm status (according to the local wind averaging convention). TCs whose intensity exceeds 119 km h^{-1} (74 mph) are classified as hurricanes in the Atlantic and eastern Pacific basins and as typhoons in the western North Pacific. Elsewhere, they are simply known as "severe tropical cyclones".

TCs are a natural part of the tropical climate system, occurring in all tropical ocean basins, with the exception of the South Atlantic (Fig. 2), although rare storms in the South Atlantic with tropical characteristics are observed. TCs have impacted the course of history, scattering and damaging Christopher Columbus' fleet in his fourth Caribbean voyage (and sinking the Spanish treasure fleet) in 1502, and thwarting the attempts of Kublai Khan to invade Japan in 1266 (Hatada [35]; Yanai [36]). As a result, TCs have inspired awe, curiosity, and, more recently, research.

Due to the differing sense of cyclonic flow across the equator, TC wind and cloud patterns are reflected for storms north and south of the equator: TCs spin counterclockwise in the northern hemisphere and clockwise in the southern hemisphere, with corresponding variations in their spiral rainband structure. In a TC, the wind flows inward cyclonically at lower levels, spiraling upward in the zones of deep convection (the central eyewall or the spiral rainbands), ultimately spiraling outward aloft, just below the tropopause (Fig. 3). Emanuel [38] closes this cycle in his theoretical model of the TC as a Carnot engine by hypothesizing a sinking branch of air far from the storm center, which ultimately recycles as inflowing air

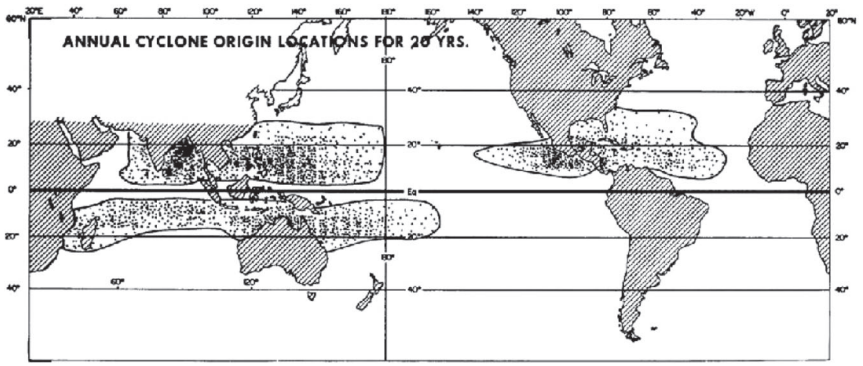

Figure 2: Global distribution of tropical cyclogenesis locations for a 20-year period (reproduced from Gray [37]).

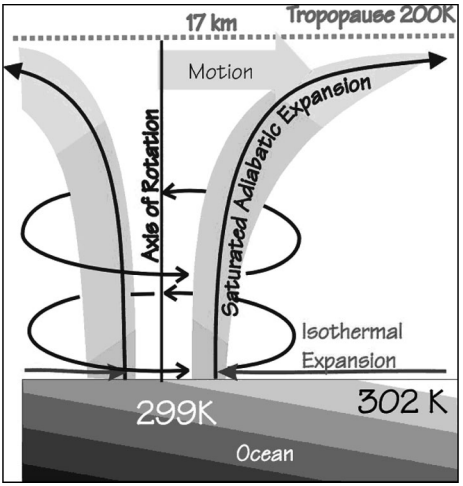

Figure 3: Schematic of the three-dimensional wind flow patterns in a typical TC (Hugh Willoughby, 2002, personal communication).

near the surface. Inflowing air is approximately isothermal, but increases its moist entropy via evaporation at the surface and decreasing pressure as it approaches the storm center.

The pattern of moist convection evident from satellite imagery is one of the most recognizable features of a TC. Four infrared satellite images for Hurricane Floyd (1999) depict the storm structure at different stages of its life cycle (Fig. 4). The clear region in the center of a mature tropical storm is known as the eye and is relatively calm with light winds and the lowest surface pressure. An organized band of thunderstorms immediately surrounds this calm center: this is the eyewall and the strongest winds are to be found on the inner flank of this thunderstorm annulus (Fig. 5).

3 Atlantic TC and ET climatology

An average of 10 named tropical storms (five hurricanes) form in the North Atlantic annually. As few as four tropical storms [in 1983] (two hurricanes [in 1982]), and as many as 21 tropical storms [in 1933] (12 hurricanes [in 1969]) have been recorded in individual years (Neumann *et al*. [40]). The earliest tropical storm formation occurred in April 2003, when Tropical Storm Ana evolved from an initially subtropical cyclone, although the hurricane season in the Atlantic, Caribbean, and Gulf of Mexico runs from June 1 to November 30. In addition, the 2003 season provided multiple landfalls (Fabian, Isabel, Juan) and ended with a rare December storm (TC Peter).

Gray [41, 42] documented six necessary (but not sufficient) conditions for tropical cyclogenesis: (i) ocean temperatures exceeding 26.5°C to a depth of 60 m; (ii) moist mid-troposphere; (iii) conditional instability; (iv) enhanced low-level

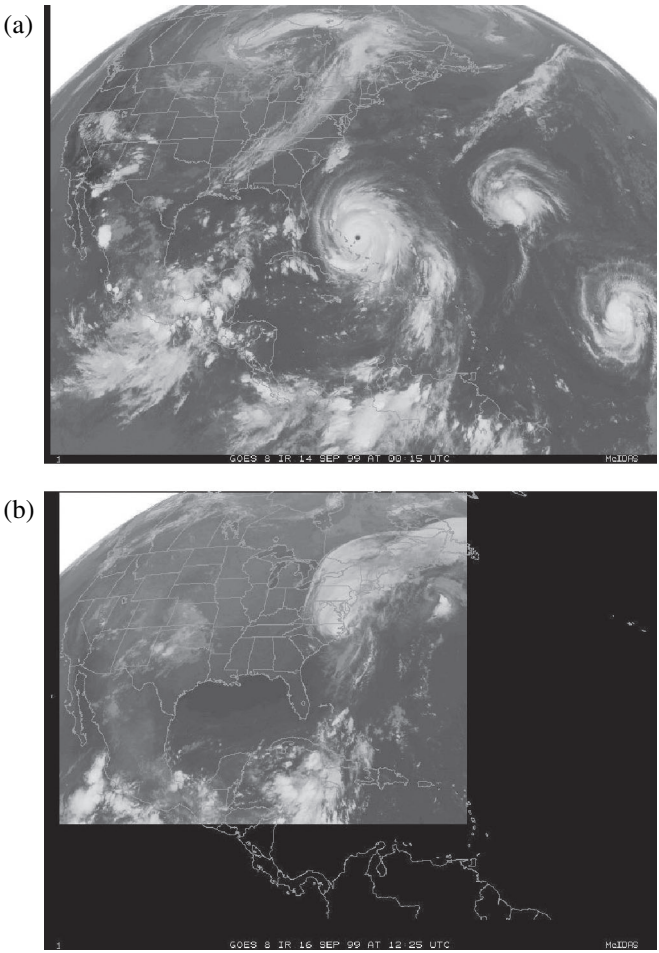

Figure 4: Hurricane Floyd (1999) GOES-8 infrared satellite imagery: (a) 0000 UTC September 14 (near peak tropical intensity), (b) 1200 UTC September 16 (ET commenced), (c) 1200 UTC September 17 (ET completed), and (d) 0000 UTC September 19 (EC over Canada).

relative vorticity; (v) weak vertical shear of the horizontal winds between 850 and 300 hPa in the genesis region, with enhanced easterly shear poleward and westerly shear equatorward; (vi) location at least 5° latitude from the equator. The seasonal evolution of these parameters explains the August through October peak in genesis frequency: the vertical wind shear tends to be weaker earlier in the season, whereas the thermal inertia of the ocean means that higher ocean temperatures and a more conditionally unstable atmosphere lag the solar peak and occur later in the season. The requirement for enhanced low-level relative vorticity is equivalent to the need for an incipient disturbance which will reduce the

(c)

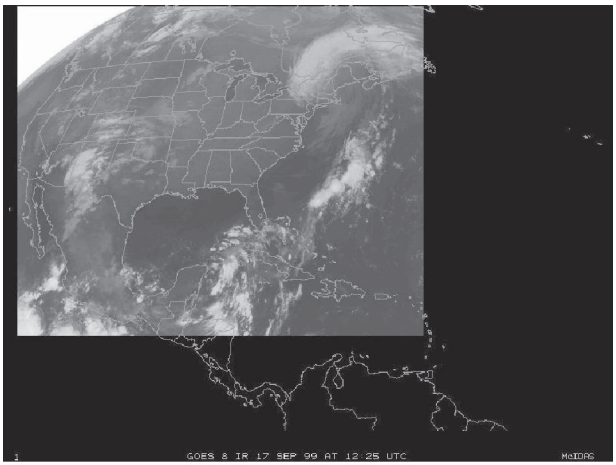

(d)

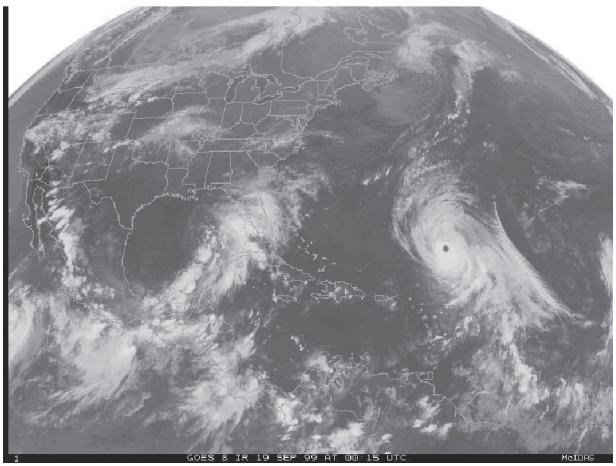

Figure 4 (*continued*)

local Rossby radius of deformation and concentrate the convective heating locally, dropping the surface pressure of the developing system and thereby enhancing the near-surface winds. In the frictional boundary layer, the increase in surface winds results in a concomitant increase in the frictional moisture convergence (whether by locally enhanced surface evaporation or radial import) which feeds the deep convection in a positive feedback cycle. Incipient disturbances may be African easterly waves (Molinari *et al*. [43]), other equatorial and near-equatorial waves (Dickinson and Molinari [44]), mesoscale convective complexes (Bister and Emanuel [45]) or subtropical low pressure systems (Bosart and Bartlo [7]). The Madden Julian Oscillation modulates the organized convection in the Atlantic basin (Evans and Jaskiewicz [46]), contributing to the intraseasonal variability of tropical cyclogenesis.

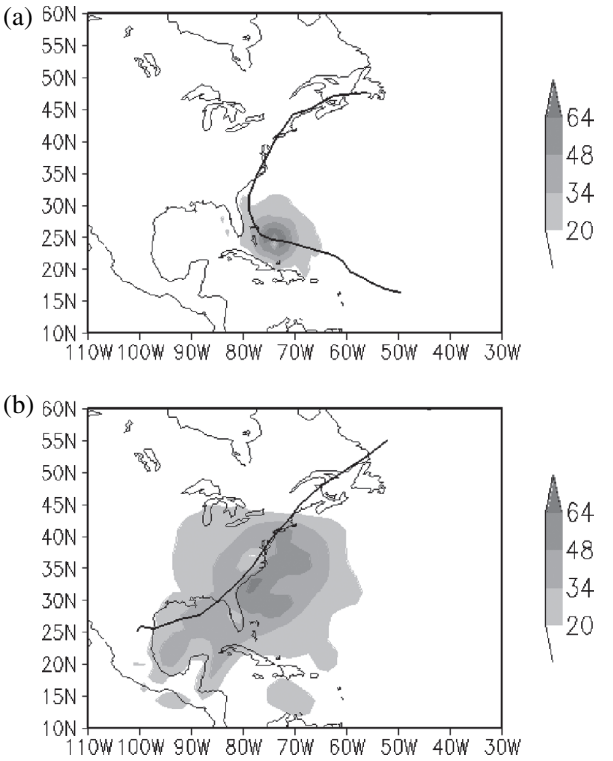

Figure 5: Comparison of 10 m wind speed distributions in examples of a typical TC and EC. Pictured are (a) Hurricane Floyd at 0000 UTC September 14, 1999 [NOGAPS 1° analysis]; (b) the "Blizzard of 1993" at 1200 UTC March 13, (NCEP/NCAR 2.5° reanalysis; Kalnay *et al.* [39]). Wind speed shading (light to dark) corresponds to winds in excess of 20 kt (37 km h^{-1}), 34 kt (63 km h^{-1}), 48 kt (89 km h^{-1}), and 67 kt (124 km h^{-1}). Note the expanded maximum wind radius of the EC (b) compared with that of the TC.

Forty-six percent of the named Atlantic tropical storms ultimately undergo ET, as defined by the National Hurricane Center (NHC) (Hart and Evans [10]). Since 1950, up to 70% and as few as 30% of these storms in a given season have been observed to undergo ET, with a standard deviation of 12%. Linear correlations with several conventional measures of climatological variability in the North Atlantic (PNA, NAO, SOI) individually describe no more than about 10% of the observed year-to-year variability. Thus, the likelihood of ET in a particular season is not readily tied to one of these measures of teleconnections. This suggests that local effects, or perhaps spatial and temporal phasing between independent systems, play a major role in determining the individual storm's potential for transition (Hart and Evans [10]).

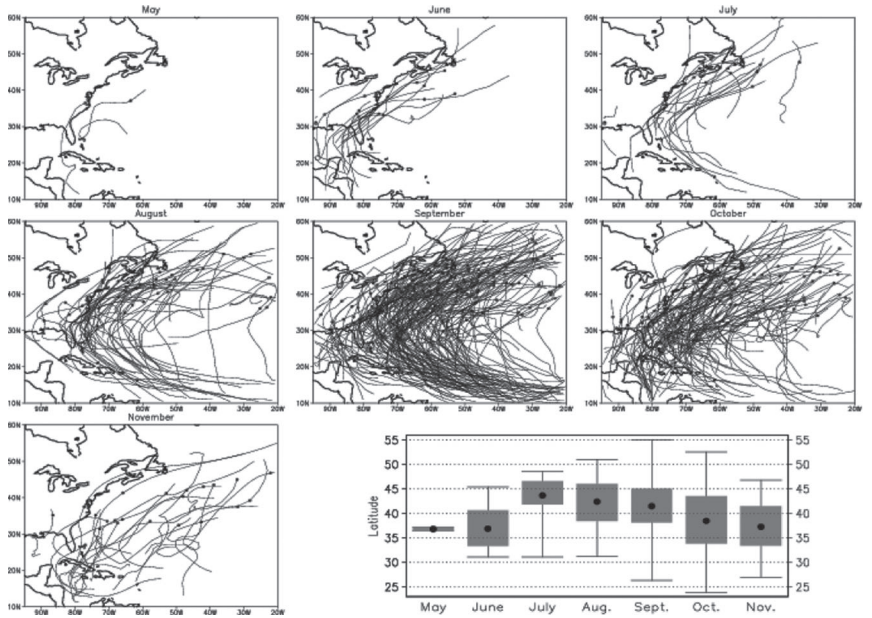

Figure 6: Tracks of extratropically transitioning North Atlantic TCs by month. Dots represent the point of transition as defined by NHC. The monthly range of latitudes over which ET has been observed is depicted in the bar chart: solid circles denote the mean transition location for each month; lighter bars represent the first and third quartiles of the transition latitudes; the horizontal bars beyond these are the extreme latitudes of observed transition. Reproduced from Hart and Evans [10].

Extratropically transitioning TCs represent almost 50% of landfalling TCs on the east coasts of the United States and Canada, and the west coast of Europe, combined (Hart and Evans [10]). The likelihood of ET increases through the tropical storm season, with a peak of 50% in October (48% in September and less than 40% in all other months) (Fig. 6). The coastal Atlantic areas most likely to be impacted by a transitioning TC are the northeast United States and the Canadian Maritimes (1–2 storms per year), and Western Europe (once every 1–2 years) (Fig. 7).

Hart and Evans [10] evaluated storm intensity changes during and after ET of the 61 transitioning tropical storms in 1979–1993. While it is extremely rare for a transitioning TC to regain its peak tropical intensity in its extratropical phase (Fig. 8a and b), 51% of ET cases underwent post-transition intensification. Over 60% of cyclones that underwent post-transition intensification originated south of 20°N (Fig. 8c), although only 52% of Atlantic storms from 1948–2000 formed in this zonal belt. In contrast, 90% of TCs that underwent post-transition decay originated north of 20°N (Fig. 8d), suggesting that strong baroclinic characteristics during formation hinder post-transition intensification and shorten the post-transition

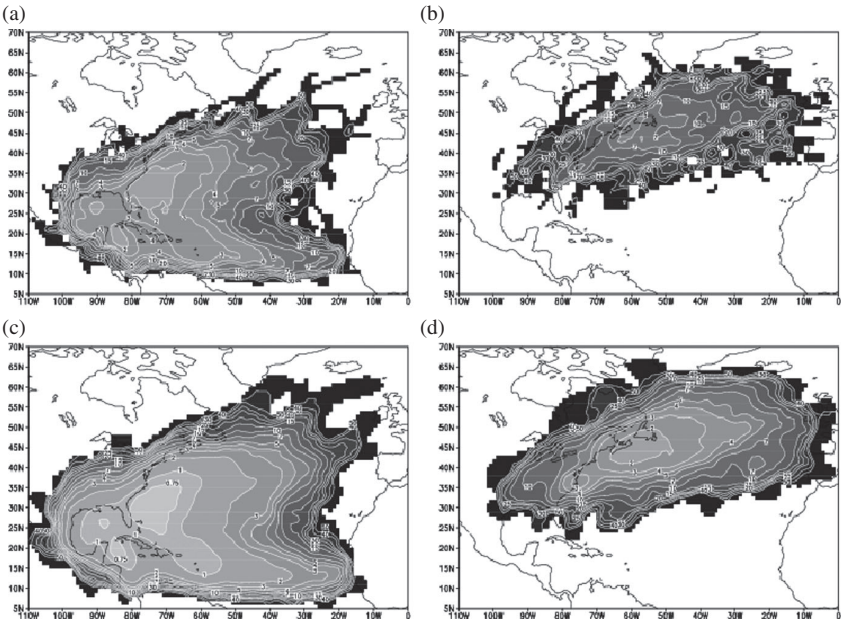

Figure 7: Mean return period in years for passage of a storm within a chosen distance of a location: (a) TC within 110 km (60 n/mi); (b) ET within 110 km; (c) TC within 300 km. (d) ET within 300 km. Figures are based on NHC best tracks from 1899–1996. Reproduced from Hart and Evans [10].

life of the ET system. Some environmental factors that modulate both the peak intensity and the likelihood of transition are explored in the next section.

4 Intraseasonal and interbasin variation in ET and proposed favorable environments

Expressed as a percentage of annual tropical storms, the Atlantic Ocean is the basin in which ET is most frequent: 46% of Atlantic TCs undergo ET (Hart and Evans [10]), while only 27% of western North Pacific storms transition. However, the much higher incidence of tropical storms in the western North Pacific basin makes it the most frequent location for ET, as noted by Klein *et al*. [22]. In the South Indian Ocean (Foley and Hanstrum [24]) and South Pacific (Sinclair [23]), ETs occur relatively infrequently, involving only 10% of tropical storms, and is not recorded in the North Indian Ocean (e.g. Grandau and Engel [47]).

Hart and Evans [10] documented the seasonal cycle of transition location and frequency in the Atlantic. They attribute this intraseasonal variation in ET latitude as the result of competing support for TC and EC cyclone development. ET occurs over the latitude range 24°N–55°N, with the highest incidence between

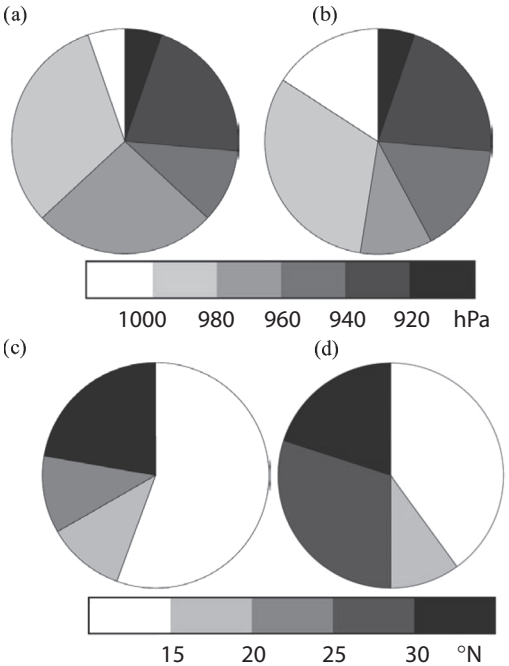

Figure 8: Characteristics of storms that go on to transition: pie charts of (a) peak tropical intensity and (b) peak post-transition intensity. Genesis latitudes for (c) reintensifying storms and (d) weakening storms.

35°N–45°N (Fig. 6). Transition occurs at lower latitudes at the beginning and end of the season, and at higher latitudes during the tropical season peak in August and September.

The peak seasonal frequency of ET occurs in September and October, when (on average) storm tracks are predominantly confined to environments that are either tropically or baroclinically supportive for development (Fig. 9). The delayed warming of the Atlantic Ocean allows the location of transition to shift northward late in the season, since the critical threshold for tropical development pushes northward. Conversely, the climatologically favored region for baroclinic development expands southward late in the season, pinching off the oceanic surface area over which tropical development can occur (Hart and Evans [10]). The relative positions of these two areas define the typical life cycle of a transitioning TC: tropical intensification, tropical decay, extratropical transition and intensification, occlusion. This seasonal tension between development regions was demonstrated using ECMWF reanalysis data for the 1985 season by Hart and Evans [10]. Global maps of these analyses have been calculated using the NCEP 2.5° × 2.5° reanalyses data of Kalnay *et al*. [39] (Fig. 9).

The intraseasonal variation evident in the North Atlantic is reproduced in the western North Pacific and is hinted at in the North and South Indian Oceans.

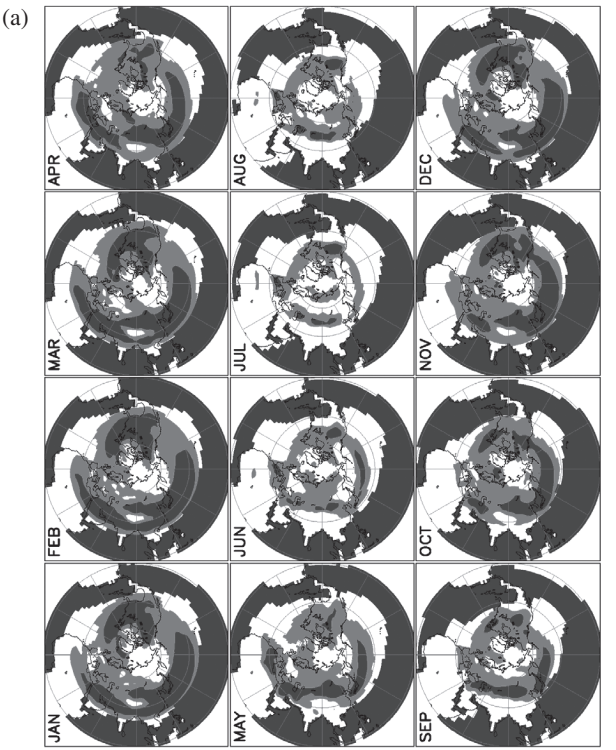

Figure 9: Comparison of the monthly mean distribution of geographic regions supporting tropical and baroclinic storm development in (a) the northern hemisphere and (b) the southern hemisphere. Regions of SST $> 28°$C have dark shading; light (medium) shading indicates regions in which the Eady baroclinic growth rate of the most unstable mode is greater than $0.25\,\text{day}^{-1}$ ($0.5\,\text{day}^{-1}$). Fields are calculated from 1982–2001 NCEP/NCAR $2.5° \times 2.5°$ monthly mean reanalyses generated by Kalnay *et al*. [39], and so probably underestimate extreme values.

The potential for ET in the North Indian Ocean (Bay of Bengal, Fig. 9a) is strongest in March, April, and November, consistent with the dual TC seasons experienced in this part of the globe. Based on this diagnostic in the southern hemisphere (Fig. 9b), the most likely months for ET off the Western Australian coast are November, April, and May: the transition months for the monsoon season there.

A storm-centered composite of the synoptic environment at the time of ET onset was calculated for a set of 11 cases of North Atlantic ET from 1998–2002. Maps of 300 hPa PV and ϑ_e (Fig. 10a) demonstrate that the transitioning storm is still distinct from the trough to its west at the time of ET onset. Using the 1PVU threshold as a measure of each system's boundary, it is clear that these systems are less than $10°$ apart at the time of transition. The TC is still warm cored, but is beginning to distort

(b)

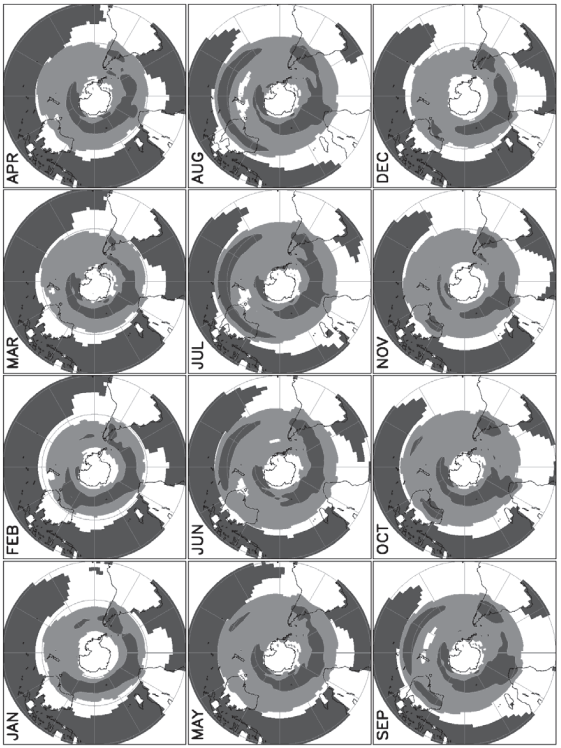

Figure 9 (*continued*)

parallel to the trough axis (NE–SW tilt evident in the storm-centered ϑ_e contours and shading of 0.5PVU region in Fig. 10a). Comparison of the upper PV and the 1000–500 hPa thickness contours (Fig. 10b) reinforces the independence of the TC and the approaching trough: the TC is still embedded in the tropical environment, although its low-level wind field is clearly beginning to distort. A much broader region of strong winds at 925 hPa is evident to the east of the TC than to its west.

5 A typical Atlantic ET case study: Hurricane Floyd (1999)

Hurricane Floyd (1999) was the deadliest US hurricane since Agnes in 1972, with 56 deaths in the United States and one on the Grand Bahama Island attributed to this storm. Floyd was almost a Category 5 hurricane when it passed just to the north and east of the central and northern Bahama islands. Over 50% of the fatalities occurred *after* Floyd made landfall in North Carolina, predominantly due to drowning in freshwater flooding (Lawrence *et al*. [48]). Floyd continued up the coast into the mid-Atlantic and New England regions, now as an extratropically transitioning system. Floyd rained heavily in this region, leaving a further trail of flooding and fatalities in its wake. Total damage estimates for the United States range from

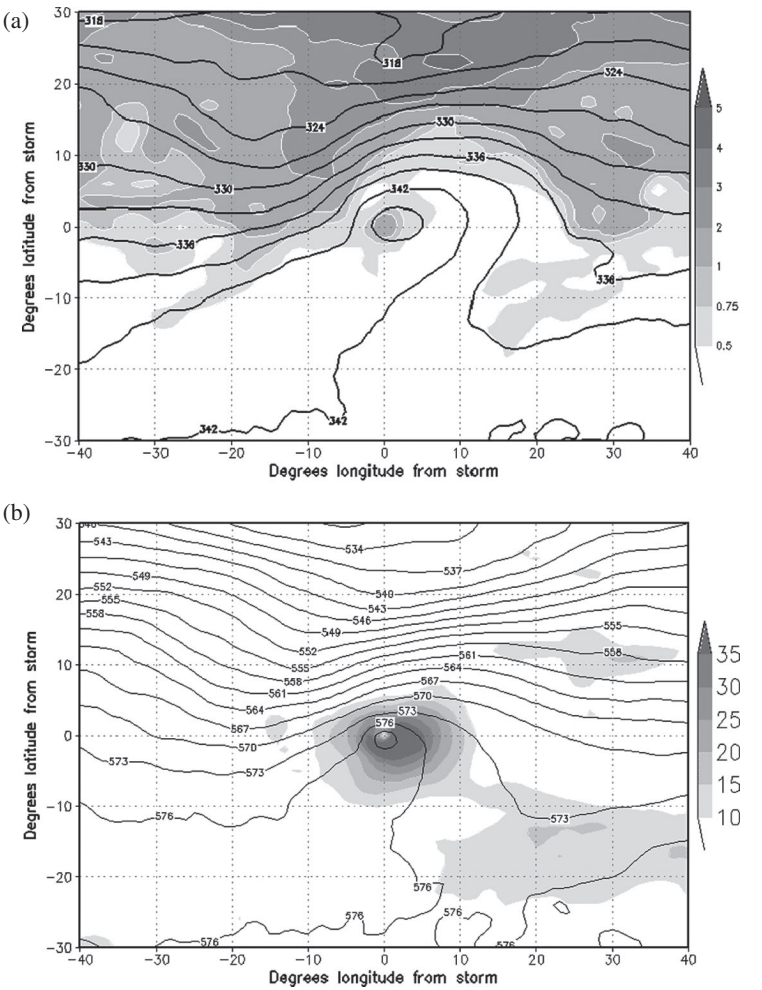

Figure 10: Storm-centered composite synoptic environment at the time of ET onset for 11 cases of North Atlantic ET: (a) 300 hPa PV (PVU; shading PV > 0.25, 0.5, 0.75, 1.0, 2.0, 3.0) and ϑ_e (contoured every 3 K); (b) 1000–500 hPa thickness (contoured every 3 dm) and 925 hPa wind speed (kt; shaded for: > 10 kt, 15 kt, 20 kt, 25 kt, 30 kt, 35 kt). Fields are from the NCEP AVN model analyses.

US$3–6 billion or more (Pasch *et al*. [49]). After being declared extratropical, Floyd continued into the Canadian Maritimes, reintensifying and causing further damage.

The evolution of Hurricane Floyd (1999) from an intense TC into an EC is described here as a typical example of ET. Floyd (1999) represents a case where ET occurs relatively quickly, with a hybrid cyclone phase (frontal warm core) of

approximately 24 h, compared with the mean transition period of 33.4 h identified by Evans and Hart [11]. Floyd had its beginning as Tropical Depression Eight, which developed from an unremarkable easterly wave originating in the Cape Verde region. It was identified at 1800UTC on September 7, 1999 and was named Tropical Storm Floyd at 0600UTC on September 8, 1999 (Lawrence *et al*. [48]). At this time, Floyd was located about 75 nmi (1400 km) to the east of the Leeward Islands. As it drifted west–northwest, Floyd slowly intensified, reaching hurricane strength at 1200UTC on September 10, now about 200 nmi (370 km) to the east–northeast of the Leeward Islands (Pasch *et al*. [49]).

A strengthening ridge to the north of Floyd resulted in a turn to the west early on the 12th. In the subsequent 24 h, the central pressure dropped rapidly by about 40 hPa and the maximum sustained winds increased from 95 knots to 135 knots (i.e. 136–250 km h^{-1}). Hurricane Floyd reached its peak tropical intensity of 921 hPa (135 kt, 250 km h^{-1}) at 1200UTC on September 13, 1999, as a symmetric warm-cored TC and remained an intense Category 4 hurricane for about 12 h (Pasch *et al*. [49]). It made landfall twice in the central and northern Bahamas on September 13 and 14, undergoing an eyewall replacement cycle. Floyd was a large, symmetric tropical system at this time, located well ahead of the approaching midlatitude trough in a low shear zone (Figs 4a and 11a).

To this time, although Hurricane Floyd had undergone a classical hurricane development, it subsequently began to weaken slowly; [48]). As an approaching trough eroded the ridge to its north, Floyd gradually turned northward and propagated parallel to the Florida coast for most of September 15. Around 0630 UTC on September 16 Floyd made landfall near Cape Fear, North Carolina (167 km h^{-1} peak winds) as a strong trough approached from the west (Fig. 11b). A number of tornadoes were reported in North Carolina associated with the storm. Storm surges as high as 9–10 feet (2.75–3.1 m) were reported along the North Carolina coast (Lawrence *et al*. [48]) as Floyd came ashore. Although it was moving rapidly ahead of the approaching trough and remained offshore, rainfall totals exceeding 12 inches (30.5 cm) were recorded in North Carolina, Virginia, Maryland, Delaware, New Jersey, and New York.

Floyd began its transition to an EC as it made landfall, acquiring frontal characteristics, shown in Fig. 4b (Evans and Hart [11]). The evolution of the transitioning Hurricane Floyd as a hybrid cyclone, having characteristics of both tropical and extratropical systems, is apparent in satellite imagery (Fig. 4b and c) and is also well documented in the evolving potential vorticity and thickness analyses of Fig. 11. By 1200 on UTC September 16, ET had commenced: Floyd had begun to interact with the positively tilted midlatitude trough to its northwest (Fig. 11b). The comma-shaped cloud signature associated with Floyd was nearly confined to the north and northwest of the center (Atallah and Bosart [13]), with a weak frontal zone evident offshore (Fig. 4b). Floyd was downgraded to a tropical storm (974 hPa, 60 kt or 111 km h^{-1}) at 1800 UTC on September 16. Floyd completed ET, acquiring a cold-core structure, at 1200 UTC on September 17 just prior to making landfall in Canada about 4 h later (Lawrence *et al*. [48]). Upon completion of the ET process, Floyd could be identified as a classic comma pattern in the IR satellite imagery

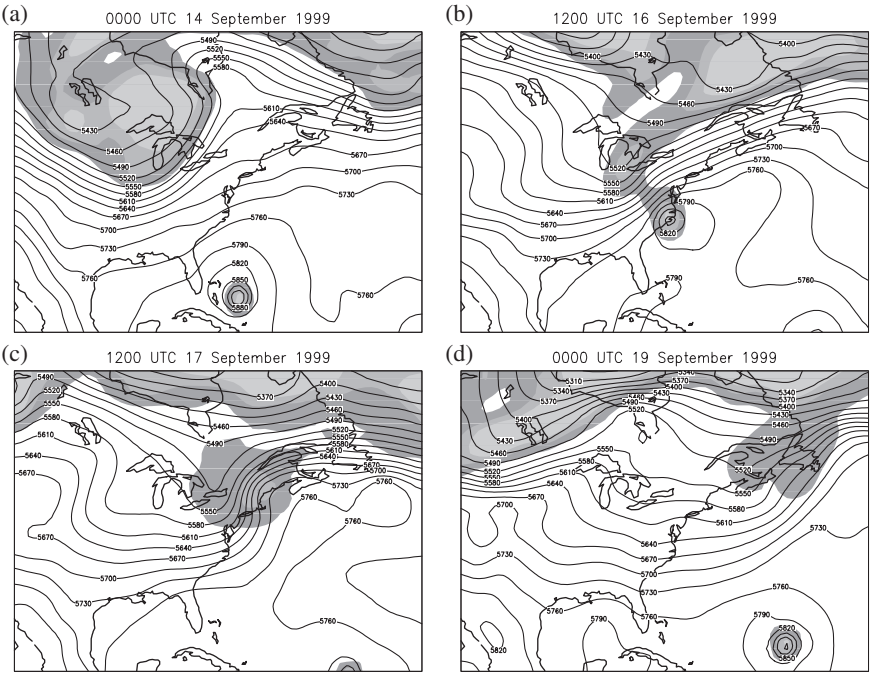

Figure 11: Evolution of Hurricane Floyd (1999), depicted through 325 K isentropic PV (shaded at 1, 2, and 3PVU) and 1000–5000 hPa thickness (contoured every 30 m) analyses from NOGAPS 1° × 1° initialization fields. Times plotted correspond to the satellite imagery in Fig. 4: (a) 0000 UTC September 14 (near peak tropical intensity); (b) 1200 UTC September 16 (ET commenced); (c) 1200 UTC September 17 (ET completed); (d) 0000 UTC September 19 (EC over Canada). Reproduced from Evans and Hart [11].

(Fig. 4c), with the strongest convective activity along a front far to the south of the system center. The PV maximum (>2 PVU) associated with Floyd was located in the baroclinic zone ahead of the weakening approaching trough (Fig. 11c). By 0000 UTC on September 19, Floyd was a weak EC with an intense tropical storm located at the southern tip of the trailing surface front (Fig. 4d). Although it was a baroclinic system when it made landfall in Canada, Floyd was still an intense system with 984 hPa central pressure and 45 kt (83 km h^{-1}) peak winds. Thereafter, the cyclone intensified as an EC until September 20, and ultimately merged with another preexisting EC (Evans and Hart [11]).

Throughout its interaction with Floyd, the midlatitude trough underwent a structural evolution reminiscent of the LC1 cycle of Thorncroft *et al*. [50] in which the trough is modulated by a larger-scale anticyclonic environmental shear, as opposed to the cyclonically sheared environment of the LC2 partition. The initially broad,

negatively tilted (northwest–southeast) trough evident in Fig. 11a (at 0000 on UTC September 14) became more narrow and acquired a positive tilt by 1200 UTC on September 16 (Fig. 11b) as it interacted with Floyd. By the time of ET completion (1200 UTC on September 17), the trough experienced further weakening and regained a neutral tilt (Fig. 11c) consistent with the southwest–northeast orientation of the jet (Fig. 11c), suggested by Thorncroft *et al*. [50]. With the progressive demise of EC Floyd, the trough continued its poleward contraction as it moved eastward across the North Atlantic (Fig. 11d). If one accepts that this trough evolution is representative of an LC1 life cycle, it can be argued that development of an EC should have been expected in the geographic area where Floyd underwent transition. However, one could also argue that the presence of a large tropical system such as Floyd should be expected to modulate the trough environment, providing an anticyclonic latitudinal shear—or enhancing a preexisting shear zone—ahead of the tropical storm. Therefore, Floyd modified the trough life cycle and the mutual interactions of Floyd and the trough led to both the LC1-type trough evolution and the ET of Floyd. Thus, the chicken and egg cannot be easily distinguished in this case!

6 Operational definitions of ET onset and completion

As noted in Section 4, ET occurs in almost all tropical storm basins, yet no universally accepted definition of extratropical transition of TCs presently exists (Malmquist [51]). Forecasters have traditionally used subjective assessments of the effects of a storm's passage over colder waters and the asymmetry of its cloud shield to determine the onset and completion of transition, yet weakening or recurving storms may also exhibit these characteristics (L. Avila 1999, personal communication). Evans and Hart [11] proposed objective diagnostics for ET onset and completion based on the CPS of Hart [34]. Here we contrast these "traditional" and objective approaches to diagnosing ET onset and completion. To do this, we must first review the CPS (Hart [34]) and its relationship to storm structure evolution. We also make comparisons with the satellite-based diagnosis of storm evolution, including the ET process, proposed by Klein *et al*. [22].

TCs are compact weather systems, with relatively symmetric cloud structures and their most intense winds at low levels, close to the storm center. Extratropical transitioning TCs evolve from this structure to become fast moving ($>10\,\mathrm{m\,s^{-1}}$), highly asymmetric systems, in which the peak low-level winds are typically much reduced, whereas the area of gale or storm force winds is often vastly increased. The maximum winds in an EC are found aloft. Thus, to describe the onset and completion of ET comprehensively, measures of both storm symmetry and wind structure must be included—either explicitly or implicitly.

6.1 Identification of ET onset

As the ET process begins, a given storm becomes increasingly asymmetric, due to low-level frontogenesis typically resulting from interaction with a midlatitude

trough (Evans and Hart [11]; Jones *et al*. [12]; Harr and Elsberry [20]; Klein *et al*. [22]; Foley and Hanstrum [24]). This increase in asymmetry is the key in detecting the onset of transition, but does not guarantee that the system will complete transition—many TCs commence ET, but decay before completing their evolution into a fully cold-core cyclone. In the case of Hurricane Floyd, the comma-shaped cloud signature and associated frontogenesis were obvious signs of a breakdown in storm symmetry, as the storm began transition.

6.2 Identification of ET evolution and completion

Tropical storms that remain coherent and persist in becoming increasingly asymmetric are promising candidates for ET. However, some systems in fact do revert to purely tropical structure after they move out of a strongly forced environment. Completion of the ET process signifies that the tropical system has developed mid-latitude storm characteristics, in particular the development of a cold-core thermal wind structure (geostrophic wind speed increasing with height), noted by Evans and Hart [11] and Jones *et al*. [12]. In the case of Floyd, it never recovered its structural symmetry; rather, as transition progressed it began to expand in size and continued to increase in asymmetry with peak winds to the right of the track and with a large area of heavy rain to the left of the track. As a further possible condition, Klein *et al*. [22] require that the storm reintensify (in terms of pressure), although classification of ET by the National Hurricane Center [NHC/NWS] is not dependent on this reintensification (L. Avila 1999, personal communication). A storm may continue to decay after recurvature, but its changed structure will be signified by its reclassification as "extratropical". In the context of operational forecasting, it is important to recognize the evolution in the storm structure because it indicates changes in the types and locations of significant weather that one could expect.

6.3 Definition of ET onset and completion using the CPS

The synoptic fields and satellite imagery used to infer transition in the previous sections are extremely valuable, but another tool has been developed recently for identifying ET—and other structural changes for the full range of synoptic cyclones. This tool is known as the cyclone phase space, or CPS (Hart [34]). The CPS is a three-parameter summary of fundamental storm structure characteristics necessary to distinguish between TC and EC types. The three parameters are calculated over a 500 km radius region centered on the surface low position (Fig. 12). They are: B, the "lower tropospheric" (900–600 hPa) thickness asymmetry; $-V_T^L$, the lower tropospheric (900–600 hPa) thermal wind; and $-V_T^U$, the upper tropospheric (600–300 hPa) thermal wind. Evans and Hart [11] demonstrated the value of this framework for discerning the onset and completion of ET. They defined ET onset as increasing asymmetry, with B exceeding the value of 10 m, which is characteristic of tropical storms and hurricanes. Once the storm has begun to lose symmetry, its lower tropospheric warm core weakens, and it

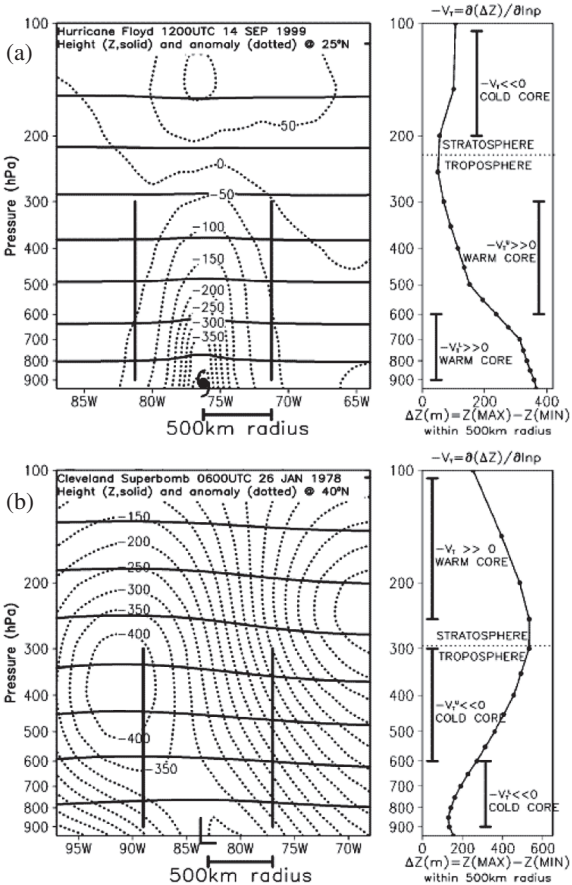

Figure 12: Comparison of radial/height thermal structure in (a) a typical TC, Hurricane Floyd (1999); (b) a typical (strong) EC, the Cleveland "superbomb" of 1978. Note the asymmetry of the EC compared with the TC. The surface low and 500 km radius are indicated. The vertical distribution of the peak height anomaly from the zonal mean at each level (indicative of the thermal wind) is plotted in the right panel in each case Reproduced from Hart [34].

typically transitions to cold core within about 24 h. ET completion is defined as the time at which $-V_T^L$ becomes negative, i.e. the system becomes cold core (Evans and Hart [11]).

To explore the differences in storm evolution for a range of life cycles, we first revisit the case of Hurricane Floyd in terms of the CPS diagnostic. Next, we examine two other cases: decaying tropical storm Hernan (2002) and the ET experience of Bonnie (1998), in terms of CPS, sea surface temperature (SST), and infrared satellite imagery.

6.3.1 Hurricane Floyd (1999)

The structural evolution of Hurricane Floyd (1999) depicted using CPS is plotted in Fig. 13: Floyd became an increasingly intense, symmetric tropical system over the week September 8–15. During this time, the symmetry parameter, B, remained near 0, while both the lower and upper tropospheric thermal wind parameters became increasingly positive, indicating a strengthening and deepening warm core. Based on the CPS onset definition for ET (Evans and Hart [11]), Floyd commenced ET around 00UTC on September 16 (Fig. 13). Once ET had begun, $-V_T^L$ began to

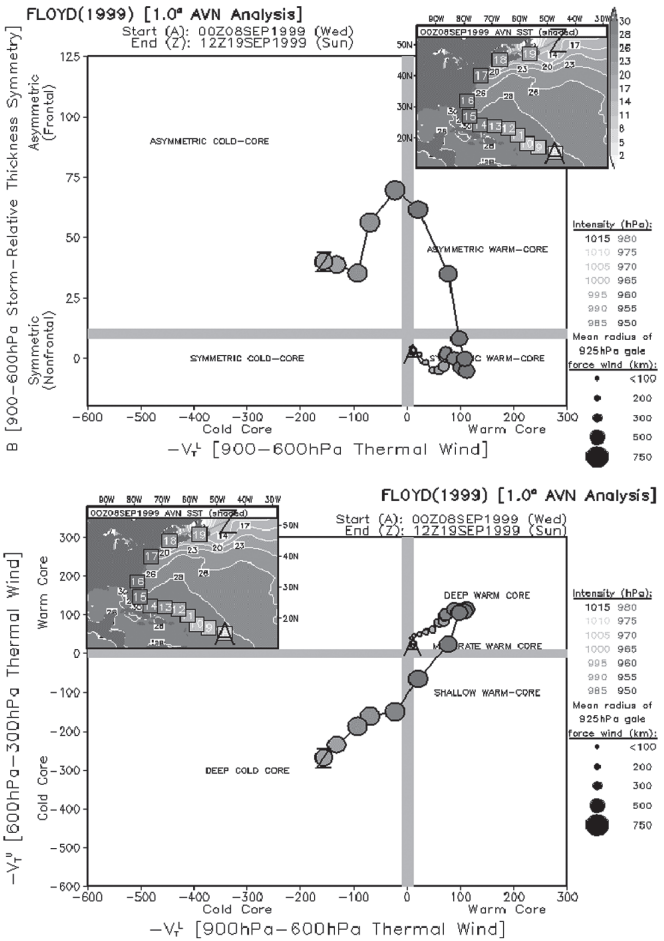

Figure 13: CPS for hurricane Floyd (1999): V_T^L versus B (top); and V_T^L versus V_T^U (bottom). The best track is plotted in the inset of each panel and begins at 0000 UTC September 8 (A), ending at 1200 UTC September 19 (Z). Size (mean 925 hPa gale force wind radius) is represented through dot size. ET commences when $B > 10$ m and completes when $-V_T^L < 0$. Reproduced from Evans and Hart [11].

decrease monotonically, eventually becoming negative at around 00UTC on the 17th and marking the completion of ET (Fig. 13).

6.3.2 Tropical storm Hernan (2002) and Hurricane Bonnie (1998)

East Pacific tropical storm Hernan (2002) did not undergo ET; rather it simply decayed. The CPS corresponding to Hernan's evolution, as well as that of Bonnie from 1998 are plotted in Fig. 14. The central pressure of Hernan intensified continually from August 28 through September 2 (Fig. 14b, shading), in agreement

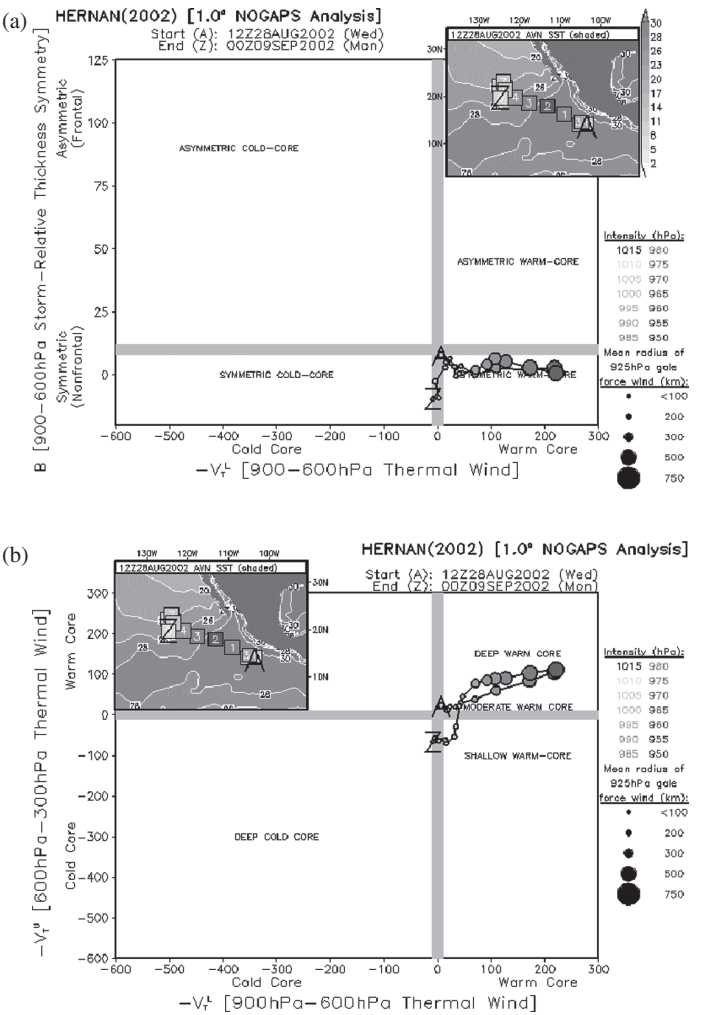

Figure 14: (a) CPS for east Pacific tropical storm Hernan (2002): V_T^L versus B; (b) V_T^L versus V_T^U. Details of the diagrams are as in Fig. 13. (c) CPS for North Atlantic Hurricane Bonnie (1998): V_T^L versus B; and (d) V_T^L versus V_T^U.

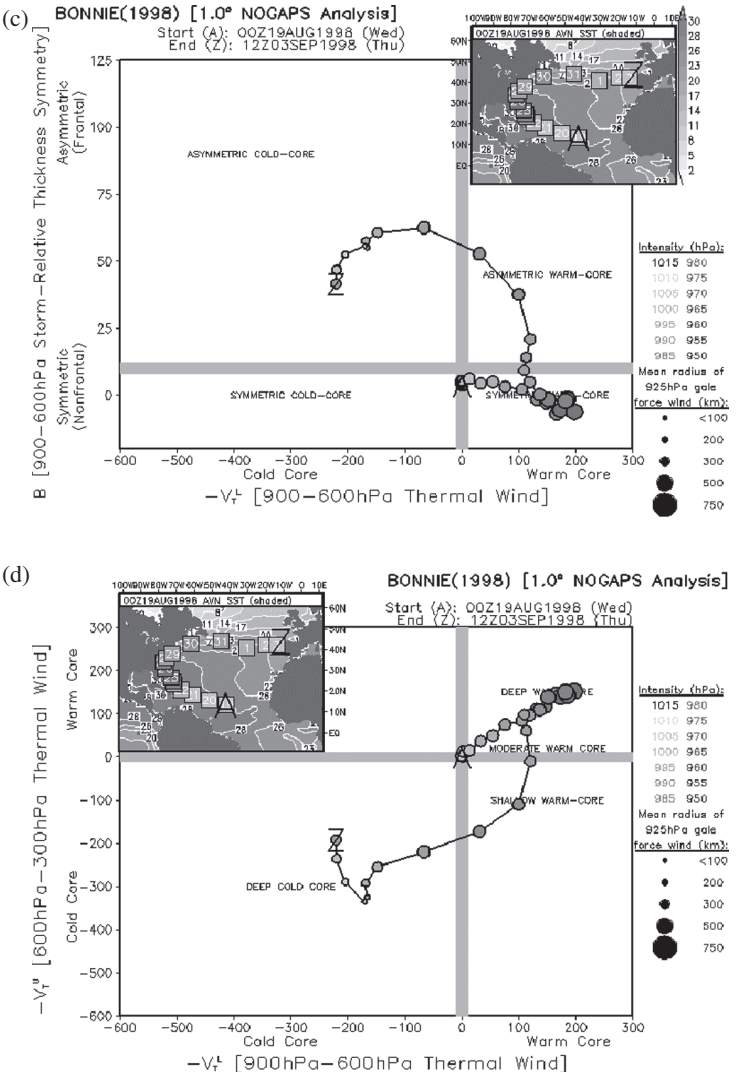

Figure 14 (*continued*)

with the tropical intensification implied by the increasingly positive thermal wind components. Over the subsequent week, Hernan slowly weakened (Fig. 14a and b). This weakening phase coincided with Hernan's movement over cooler SST < 26°C (Fig. 15a) and very weak SST gradients. Drier air is also observed intruding towards the storm center and beginning to erode the eyewall (Fig. 15b). This erosion of the cloud shield to the south was proposed by Klein *et al*. [22] as one identifier of ET, yet this case highlights the need to use this diagnostic with other ET indicators to avoid confusion between the ET process and the purely decaying cases.

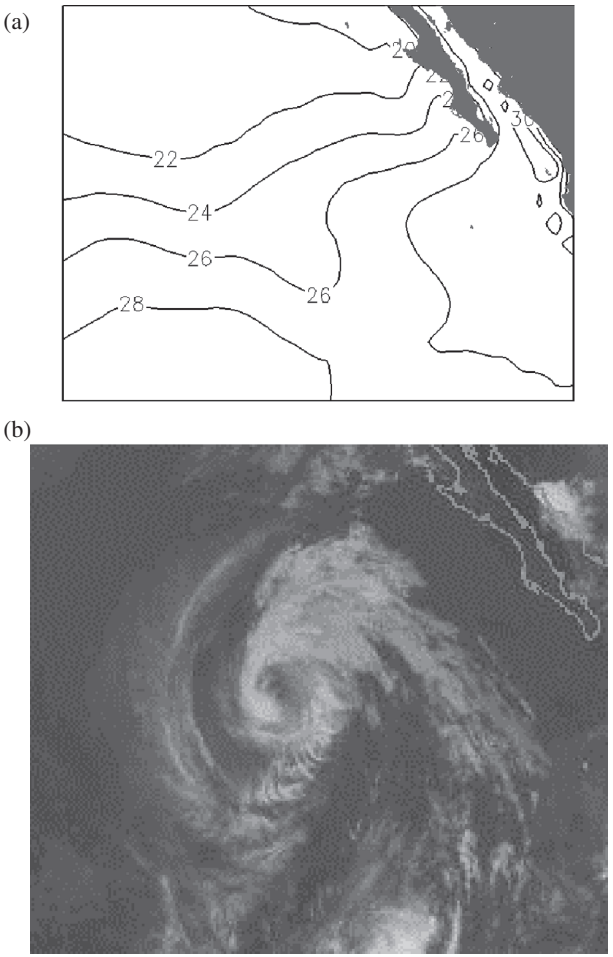

Figure 15: (a) SST and (b) GOES-8 infrared satellite imagery at 1200 UTC September 4, 2002, for decaying east Pacific tropical storm Hernan. (c) SST and (d) GOES-8 infrared satellite imagery for North Atlantic extratropically transitioning Hurricane Bonnie 1200 UTC August 29, 1998.

Both the tropical and post-tropical structural evolution of Hurricane Bonnie (1998) have much more in common with Floyd than they do with Hernan. Bonnie was an intense tropical system that remained coherent through the ET process on August 30, 1998, and continued for many days subsequent to transition, as an EC (Fig. 14c and d). While Bonnie was certainly over waters cooler than 26°C by September 29, she remained near the Gulf Stream (Fig. 15c) and so the SST gradients were much stronger than for the case of Hernan (2002). This may have allowed Bonnie to be impacted by the warmer water source, still relatively close to the south,

(c)

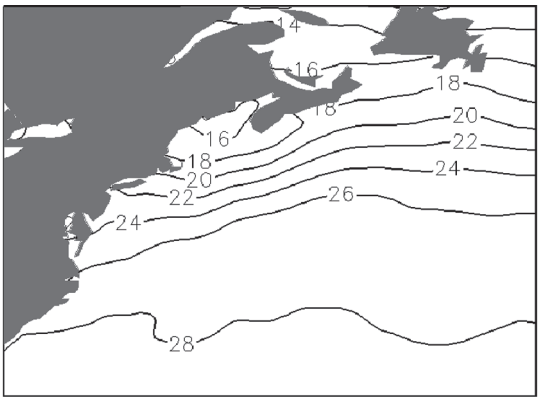

(d)

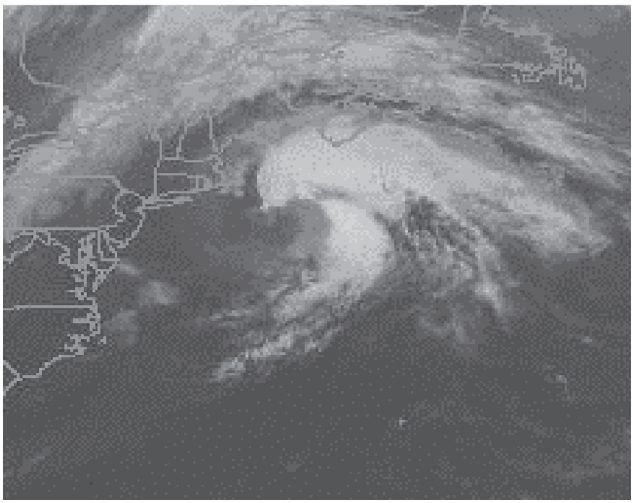

Figure 15 (*continued*)

and to modify its downstream environment somewhat through continual warm air advection (Fig. 15c). Klein *et al*.'s [22] signature erosion of the cloud shield during ET is evident near the center and to its south (Fig. 15d).

6.4 Storm life cycle mapped in terms of the CPS

Arnott *et al*. [14] have taken interpretation of the CPS one additional step. They used K-means cluster analysis to explore the temporal evolution of storm structure (characterized using the CPS) for a set of 19 ET cases. They identified seven distinct clusters representing tropical (three clusters, based on storm strength), extratropical (two clusters), transitioning (one cluster), and hybrid (one cluster) storm structures.

Arnott *et al*. [14] isolated the major path of storm structure evolution through the CPS for these 19 ET cases and calculated storm-centered composites of the synoptic environment for each cluster. The composite environment for cluster #4—the time of ET onset—is very similar to that presented in Fig. 10 (not shown; see Arnott *et al*. [14] for details).

7 Summary

Unlike the "conventional" TC, the poleward movement of an extratropically transitioning TC does not simply lead to the decay of the system as it moves into the midlatitudes. TCs undergoing ET typically weaken as they recurve (Evans and McKinley [52]), but as they move into the extratropics these systems can reintensify into intense midlatitude storms with extensive regions of intense rain and larger gale (and even hurricane) force wind areas than their tropical antecedents. The remnant TC can also provide a region of enhanced thermal contrast for the later development of an intense midlatitude storm. The rapid forward speed, the large size of their gale force wind area and intense rainfall region, and the extraordinarily large ocean waves of an ET can persist long after its "tropical storm" status has been discontinued.

ET has been identified to be prevalent across the tropical ocean basins, with the possible exception of the North Indian Ocean. Approximately half of all Atlantic and one-third of west Pacific systems undergo ET. In the Atlantic, almost 50% of these ET systems also make landfall, making ET a real concern for Atlantic hurricane forecasters. Interaction with a synoptic-scale trough is a dominant mechanism for ET, although the tropical system must be sufficiently well supported for tropical development until this time (Hart and Evans [10]).

ET is often poorly forecast by numerical forecast models, providing difficult forecast challenges to the responsible forecast centers around the globe (e.g. Rabier *et al*. [29]). A number of new diagnostics have been proposed to characterize ET: using storms from the western North Pacific, Klein *et al*. [22] have identified satellite imagery signatures and environments typical of ET cases; Evans and Hart [11] have applied the CPS (developed by Hart [34]) as a diagnostic of ET for the North Atlantic. In Atlantic ET cases, the satellite signature proposed by Klein *et al*. [22] is also evident, but it can be found in cases of tropical storms that simply decay (e.g. Hernan 2002). Arnott *et al*. [14] have used cluster analysis to discriminate objectively between different storm structure stages. Using the K-means method, they were able to reproduce the ET onset and completion thresholds arrived at subjectively by Evans and Hart [11]. Composite synoptic environments for ET developed by Arnott *et al*. [14] agree well with those presented here.

Acknowledgments

This work was supported by the NSF under grant ATM-0351926. The permission of the American Meteorological Society to reproduce Figs 6 and 7 from Hart and

Evans [10], Figs 11 and 16 from Evans and Hart [11], and Fig. 12 from Hart [34] is gratefully acknowledged. We thank Justin Arnott for preparing Fig. 8 and for helpful discussions on the storm stages. We are grateful to Prof. William Gray for permission to reproduce his work in Fig. 2.

References

[1] Tannehill, I.R., Hurricane of September 16 to 22, 1938. *Monthly Weather Review*, **66**, pp. 286–288, 1938.
[2] Pierce, C.H., The meteorological history of the New England Hurricane of September 21, 1938. *Monthly Weather Review*, **67**, pp. 237–285, 1939.
[3] Palmén, E., Vertical circulation and release of kinetic energy during the development of Hurricane Hazel into an extratropical storm. *Tellus*, **10**, pp. 1–23, 1958.
[4] Kornegay, F.C. & Vincent, D.G., Kinetic energy budget analysis during interaction of tropical storm Candy (1968) with an extratropical frontal system. *Monthly Weather Review*, **104**, pp. 849–859, 1976.
[5] DiMego, G.J. & Bosart, L.F., The transformation of tropical storm Agnes into an extratropical cyclone. Part I: The observed fields and vertical motion computations. *Monthly Weather Review*, **110**, pp. 385–411, 1982.
[6] DiMego, G.J. & Bosart, L.F., The transformation of tropical storm Agnes into an extratropical cyclone. Part II: Moisture, vorticity, and kinetic energy budgets. *Monthly Weather Review*, **110**, pp. 412–433, 1982.
[7] Bosart, L.F. & Bartlo, J.A., Tropical storm formation in a baroclinic environment. *Monthly Weather Review*, **119**, pp. 1979–2013, 1991.
[8] Bosart, L.F. & Lackmann, G.M., Post-landfall tropical cyclone reintensification in a weakly baroclinic environment: a case study of hurricane David (September 1979). *Monthly Weather Review*, **123**, pp. 3268–3291, 1995.
[9] Thorncroft, C. & Jones, S.C., The extratropical transition of hurricanes Felix and Iris in 1995. *Monthly Weather Review*, **128**, pp. 947–972, 2000.
[10] Hart, R.E. & Evans, J.L., A climatology of extratropical transition of Atlantic tropical cyclones. *Journal of Climate*, **14**, pp. 546–564, 2001.
[11] Evans, J.L. & Hart, R.E., Objective indicators of the onset and completion of extratropical transition for Atlantic tropical cyclones. *Monthly Weather Review*, **131**, pp. 909–925, 2003.
[12] Jones, S.C., Harr, P.A., Abraham, J., Bosart, L.F., Bowyer, P.J., Evans, J.L., Hanley, D.E., Hanstrum, B.N., Hart, R.E., Lalaurette, F., Sinclair, M.R., Smith, R.K. & Thorncroft, C., The extratropical transition of tropical cyclones: Forecast challenges, current understanding and future directions. *Weather and Forecasting*, **18**, pp. 1052–1092, 2003.
[13] Atallah, E. & Bosart, L.F., The extratropical transition and precipitation distribution of Hurricane Floyd (1999). *Monthly Weather Review*, **131**, pp. 1063–1081, 2003.

[14] Arnott, J.M., Evans, J.L. & Chiaromonte, F., Characterization of extratropical transition using cluster analysis. *Monthly Weather Review*, **132**, pp. 2916–2937, 2004.
[15] Sekioka, M., A hypothesis on complex of tropical and extratropical cyclones for typhoon in the middle latitudes. I. Synoptic structure of typhoon Marie passing over the Japan Sea. *Journal of the Meteorological Society of Japan*, **34**, pp. 276–287, 1956.
[16] Sekioka, M., A hypothesis on complex of tropical and extratropical cyclones for typhoon in the middle latitudes. II. Synoptic structure of typhoons Louise, Kezia, & Jane passing over the Japan Sea. *Journal of the Meteorological Society of Japan*, **34**, pp. 336–345, 1956.
[17] Sekioka, M., A hypothesis on complex of tropical and extratropical cyclones for typhoon in the middle latitudes. III. Examples of typhoon not accompanied by extratropical cyclone in the middle latitudes. *Journal of the Meteorological Society of Japan*, **35**, pp. 170–173, 1957.
[18] Matano, H. & Sekioka, M., Some aspects of extratropical transformation of a tropical cyclone. *Journal of the Meteorological Society of Japan*, **49**, pp. 736–743, 1971.
[19] Brand, S. & Guard, C.P., Extratropical storm evolution from tropical cyclones in the western North Pacific ocean. *Naval Environmental Prediction Technical Report TR 78-02*, pp. 1–20, 1978.
[20] Harr, P. & Elsberry, R.L., Extratropical transition of tropical cyclones over the western North Pacific. Part I: Evolution of structural characteristics during the transition process. *Monthly Weather Review*, **128**, pp. 2613–2633, 2000.
[21] Harr, P., Elsberry, R.L. & Hogan, T., Extratropical transition of tropical cyclones over the western North Pacific. Part II: The impact of midlatitude circulation characteristics. *Monthly Weather Review*, **128**, pp. 2634–2653, 2000.
[22] Klein, P., Harr, P. & Elsberry, R.L., Extratropical transition of western North Pacific tropical cyclones: an overview and conceptual model of the transformation stage. *Weather and Forecasting*, **15**, pp. 373–396, 2000.
[23] Sinclair, M.R., Extratropical transition of southwest Pacific tropical cyclones. Part I: Climatology and mean structure changes. *Monthly Weather Review*, **130,** pp. 590–609, 2002.
[24] Foley, G.R. & Hanstrum, B.N., The capture of tropical cyclones by cold fronts off the west coast of Australia. *Weather and Forecasting*, **9**, pp. 577–592, 1994.
[25] Prater-Mayes, B. & Evans, J.L., Sensitivity of modeled tropical cyclone track and structure of Hurricane Irene (1999) to the convection parameterization scheme. *Meteorology and Atmospheric Physics*, **80**, pp. 103–115, 2002.
[26] Evans, J.L. & Prater-Mayes, B., Factors affecting the post-transition intensification of Hurricane Irene (1999). *Monthly Weather Review*, **132**, pp. 1355–1368, 2004.

[27] Agusti-Panareda, A., Thorncroft, C.D., Craig, G.C. & Gray, S.L., The extratropical transition of hurricane Irene (1999): a potential vorticity perspective. *Quarterly Journal of the Royal Meteorological Society*, **130**, pp. 1–28, 2004.

[28] Abraham, J.D., *et al*., Extratropical transition. *Fifth WMO/ICSU Int. Workshop on Tropical Cyclones (IWTC- V), Topic 4.6*, Cairns, Australia, December 1–13, 2002.

[29] Rabier, F., Klinker, E., Courtier, P. & Hollingsworth, A., Sensitivity of forecast errors to initial conditions. *Quarterly Journal of the Royal Meteorological Society*, **122,** pp. 121–150, 1996.

[30] Bowyer, P.J., Phenomenal waves with a transitioning tropical cyclone (Luis, the Queen, and the buoys). *Preprints, 24th AMS Conference on Hurricanes and Tropical Meteorology*, Fort Lauderdale, FL, pp. 294–295, 2000.

[31] Moon, I.-J., Ginis, I., Hara, T., Tolman, H., Wright, C.W. & Walsh, E.J., Numerical simulation of sea-surface directional wave spectra under hurricane wind forcing. *Journal of Physical Oceanography*, **33**, pp. 1680–1706, 2003.

[32] MacAfee, A.W. & Bowyer, P.J., Trapped-fetch waves in a transitioning tropical cyclone (Part I—The need and the theory). *Preprints, 24th AMS Conference on Hurricanes and Tropical Meteorology*, Fort Lauderdale, FL, pp. 292–293, 2000.

[33] MacAfee, A.W. & Bowyer, P.J., Trapped-fetch waves in a transitioning tropical cyclone (Part II—Analytical and predictive model). *Preprints, 24th AMS Conference on Hurricanes and Tropical Meteorology*, Fort Lauderdale, FL, pp. 165–166, 2000.

[34] Hart, R.E., A cyclone phase space derived from thermal wind and thermal asymmetry. *Monthly Weather Review*, **131**, pp. 585–616, 2003.

[35] Hatada, T., *The Mongol Invasions* (in Japanese), Chuokoron Sha: Tokyo, 1965.

[36] Yanai, M., *English translation of the letter by the Khubilai Khan to the Japanese emperor in 1266*, Meteo 216B class notes. Available from Prof. Yanai, UCLA, 1975.

[37] Gray, W.M., Hurricanes: their formation, structure and likely role in the tropical circulation. *Meteorology Over the Tropical Oceans*, ed. D.B. Shaw, *Royal Meteorological Society*, pp. 155–218, 1979.

[38] Emanuel, K.A., Sensitivity of tropical cyclones to surface exchange coefficients and a revised steady-state model incorporating eye dynamics. *Journal of the Atmospheric Sciences*, **52**, pp. 3969–3976, 1995.

[39] Kalnay, E., Kanamitsu, M., Kistler, R., Collins, W., Deaven, D., Gandin, L., Iredell, M., Saha, S., White, G., Woollen, J., Zhu, Y., Leetmaa, A., Reynolds, B., Chelliah, M., Ebisuzaki, W., Higgins, W., Janowiak, J., Mo, K.C., Ropelewski, C., Wang, J., Jenne, R. & Joseph, D., The NCEP/NCAR 40-year reanalysis project. *Bulletin of the American Meteorological Society*, **77**, pp. 437–472, 1996.

[40] Neumann, C.J., Jarvinen, B.R., McAdie, C.J. & Elms, J.D., *Tropical Cyclones of the North Atlantic Ocean 1871–1992*. NOAA Historical Climatology Series 6–2, National Climatic Data Center. Asheville, NC, 1993.
[41] Gray, W.M., Global view of the origin of tropical disturbances and storms. *Monthly Weather Review*, **96**, pp. 669–700, 1968.
[42] Gray, W.M., Tropical cyclone genesis and intensification. *Intense Atmospheric Vortices*, eds L. Bengtsson & J. Lighthill, Springer: New York, pp. 3–20, 1982.
[43] Molinari, J., Knight, D., Dickinson, M., Vollaro, D. & Skubis, S., Potential vorticity, easterly waves and eastern Pacific tropical cyclogenesis. *Monthly Weather Review*, **125**, pp. 2699–2708, 1997.
[44] Dickinson, M. & Molinari, J., Mixed Rossby-gravity waves and western Pacific tropical cyclogenesis. Part I: Synoptic evolution. *Journal of the Atmospheric Sciences*, **59**, pp. 2183–2196, 2002.
[45] Bister, M. & Emanuel, K.A., The genesis of Hurricane Guillermo: TEXMEX analyses and a modeling study. *Monthly Weather Review*, **124**, pp. 2662–2682, 1997.
[46] Evans, J.L. & Jaskiewicz, F.A., Satellite-based monitoring of intraseasonal variations in tropical Pacific and Atlantic convection. *Geophysical Research Letters*, **28**, pp. 1511–1514, 2001.
[47] Grandau, F. & Engel, G., *JTWC 2001 Annual Tropical Cyclone Report*. Available from https://metoc.npmoc.navy.mil/jtwc/atcr/2001atcr, 2001.
[48] Lawrence, M.B., Avila, L.A., Beven, J.L., Franklin, J.L., Guiney, J.L. & Pasch, R.J., Atlantic hurricane season of 1999. *Monthly Weather Review*, **129**, pp. 3057–3084, 2001.
[49] Pasch, R.J., Kimberlain, T. & Stewart, S.R., Preliminary report on Hurricane Floyd September 7–17, 1999. National Hurricane Center, 1999 [Available from the Tropical Prediction Center, Miami, FL; also available online at http://www.nhc.noaa.gov/1999/floyd.html].
[50] Thorncroft, C.D., Hoskins, B.J. & McIntyre, M.E., Two paradigms of baroclinic wave life cycle behavior. *Quarterly Journal of the Royal Meteorological Society*, **119**, pp. 17–55, 1993.
[51] Malmquist, D. Meteorologists and insurers explore extratropical transition of tropical cyclones. *EOS*, February 16, 1999.
[52] Evans, J.L. & McKinley, K., Relative timing of tropical storm lifetime maximum intensity and track recurvature. *Meteorology and Atmospheric Physics*, **65**, pp. 241–245, 1998.